

Evaluation of Seismic Performance of PBD Optimized Steel Moment Frames by Means of Neural Network

Masood Danesh

Department of Civil Engineering, Khoy Faculty of Engineering, Urmia University, Khoy, Iran.
E-Mail: m.danesh@urmia.ac.ir

ABSTRACT

Performance-based design (PBD) is a method for structural design that accommodates different levels of structure performance against appropriate levels of earthquake intensities. On the contrary, reliability-based design (RBD) puts the reliability of the designed structure to achieve the desired performance levels as the basis of action and, unlike PBD, which utilizes deterministic design parameters, is of probabilistic geometrical and mechanical characteristics so that each of these probabilistic variables, with a specific mean and standard deviation, has a particular statistical distribution. In the present paper, 3, 6 and 12-story moment-resisting steel frames with special ductility are first optimized by using meta-heuristic optimization algorithms of PSO, ECBO, FA as well as finite difference algorithm (FDA), proposed by the author, based on the structure performance with initial cost objective function and using neural network. Thereafter, the reliability and collapse margin ratio (CMR) of the optimized frames are evaluated using the FEMA-P695 code. The obtained results show that although in terms of targeting the initial cost, the optimized frames have a structural weight nearly as low as possible; however, because of the relatively small reliability and CMR resulting from the use of deterministic design parameters by the PBD method, the frames will have a higher lifecycle cost. Therefore, in order to optimize such frames using PBD method, the use of the initial cost objective function is not recommended unless an optimal CMR value is included in the optimization constraints for their seismic performance or the optimization is performed by the RBD approach.

KEYWORDS: Structural optimization, Initial cost, Collapse margin ratio (CMR), Performance-based design, Reliability-based design, Neural network.

INTRODUCTION

Seismic design of structures was initially formed around the concepts of strength and resistance, rather than being based on deformation control. The occurrence of severe earthquakes in the United States and Japan has shown that the damages created in structures are very high despite the design of the structures according to the versions of seismic design

regulations. This made the engineering community criticize the effectiveness of the seismic design regulations and in order to reduce the seismic damages, more resistant designs should be created. This feeling finally led to the development of PBD techniques.

The concept of PBD has been introduced in recent years by using various guidelines for assessing and retrofitting existing structures and analyzing and designing new projects (Council, A.T., 1996; Provisions, 1997; Council, B.S.S., 2000; Safety, I.S.; Council, A.T., 2009; Agency, F.E.M., 2013; FEMA, 2005; Neighbors, 2012). The main purpose is to increase

Received on 23/4/2019.

Accepted for Publication on 4/7/2019.

the safety of structures against natural hazards and their predictable and reliable performance against earthquakes. In other words, structures must be able to resist earthquakes more and the vulnerability level should be reduced.

The aim of Performance-based Design Optimization (PBDO) of structures in earthquake engineering is to obtain optimal design variables that minimize an objective function, such as initial cost, lifecycle cost, geometric form,... etc. of the structure with respect to functional constraints. In this process, if design parameters, such as Young's modulus, yielding stress, strain hardening, spectral accelerations,... etc., are considered as a probabilistic variable with a specific mean, standard deviation and statistical distribution, then Reliability-based Design Optimization (RBDO) is formed.

Since static nonlinear analysis (pushover) is required to calculate the structure response at different performance levels, the overall processing time for optimization is high. To reduce high computational time and cost, neural networks are used.

In 2009, FEMA issued an instruction in the form of FEMA-P695 (Council, A.T., 2009), from which collapse safety rate is evaluated by calculating CMR and adjusting it with the consideration of design uncertainties (Adjusted Collapse Margin Ratio (ACMR)) and the probability of breaking failure criteria is obtained.

In the present paper, three moment-resisting steel frames of 3, 6 and 12 stories are first optimized by using the PBDO approach and initial cost objective function, using 4 optimization algorithms of PSO, ECBO, FA and FDA and by the help of neural network. Then, the CMR of the optimized frames is calculated. The results indicate that low reliability and CMR of the structures optimized based on the PBD approach and the initial cost objective function will probably increase the lifecycle cost of the structure.

Performance-Based Design Optimization (PBDO)

The main purpose of PBD is to empower structures

so that they can resist earthquakes better and prevent the expected level of vulnerability. Immediate Occupancy (IO), Life Safety (LS) and Collapse Prevention (CP) are considered as different performance levels in PBD codes. The IO level represents a very small damage with small local failures. At the LS level, the structure is seriously damaged, but sufficient safety is provided for residents to evacuate the building. The CP level is associated with massive plastic deformation of structural members, and the slightest increase in load or lateral displacement will result in the structure collapse. Different levels of optimal performance for different levels of earthquake depend upon the degree of importance of the structure.

Since inelastic deformations are used directly in PBD in order to identify the level of damage from severe earthquakes, a nonlinear analysis method is required to evaluate the characteristics of structure performance at different levels during earthquakes. Pushover analysis is widely accepted as an effective method for nonlinear analysis, due to its simplicity compared with nonlinear dynamic methods. The aim of pushover nonlinear static analysis is to evaluate the structural performance in terms of capacity and deformation both overall and in the members. The main output of pushover analysis is the curve of the structure inelastic capacity.

By the help of the benefits provided by static or dynamic nonlinear approaches, a highly efficient structural design can be achieved with optimization (Fragiadakis and Lagaros, 2011). For this purpose, optimization algorithms can be a very good alternative to the traditional "try and error" process in solving PBD problems. Gradient-based optimization methods have great problems, such as the necessity of forming a fixed form for the quasi-objective function in solving complex problems. In comparison with the optimization algorithms, meta-heuristic methods can be used. Widespread studies have been carried out on the PBDO of structures over the past years. Meta-heuristic methods have been used in a number of these studies. A number of papers published in this field are listed as follows:

Liu et al. (2013) designed a genetic algorithm (GA)

based on the multi-objective method of structural optimization for steel frames with regards to weight and maximum inter-story drift, at two performance levels. Fragiadakis and Lagaros (2011) presented a method based on evolution strategies (ESs) considering inelastic behavior and repair cost for determining the effects of future earthquakes during the design phase to achieve optimal design of steel structures under seismic loads. Kaveh et al. (2010) compared computational performance of the meta-heuristic Ant Colony Optimization (ACO) and Genetic Algorithm (GA) for optimal seismic design based on the frames' performance. In an interesting paper, Fragiadakis et al. (2006) presented the application of the concept of performance-based seismic design by using meta-heuristic Particle Swarm Optimization (PSO) algorithm and with the lifecycle cost objective function. In the formulae presented that are consistent with the PBD concept, the issue of seismic design has been investigated in a deterministic or probabilistic method and has been integrated with one or more objectives that represent the initial cost or costs from future earthquake damages. Gholizadeh et al. (2013) compared the computational performance of meta-heuristic algorithms of GA, PSO, ACO and harmonic search (HS) for PBDO of steel structures. This study revealed the superiority of PSO to other meta-heuristic algorithms. In newer studies, Gholizadeh (2015) and Gholizadeh and Milany (2018) presented an effective method for performing PBDO on steel structures using a combination of Modified Firefly Algorithm (MFA) and neural networks, in such a way that could predict pushover analysis results by a neural network during the optimization process and achieve significant savings in the calculation time and load of the optimization. Finally, Kaveh et al. provided the optimization of truss and steel frame using Colliding Bodies Optimization (CBO) algorithm (Kaveh and Mahdavi, 2014; Kaveh and Mahdi, 2014) and its enhanced algorithm (ECBO) (Kaveh and Ghazaan, 2014; Kaveh and Ghazaan, 2017), with multi-quasi objective function (Kaveh et al., 2012), CSS algorithm (Kaveh and Nasrollahi, 2014) and

nonlinear dynamic procedure (Kaveh et al., 2015).

Defining performance objectives is an essential part of PBDO. Performance objectives are defined as a specific level of the performance of seismic hazard level. In order to determine the performance objectives, the structural performance level must first be determined. Then, the level of seismic hazard is determined. In this paper, the performance levels of IO and CP are considered in accordance with FEMA-350 (Agency, F.E.M., 2013). The IO and CP performance levels correspond to 50% and 2% of the probability of aggression in 50 years, respectively (Provisions, 1997).

Another part of the PBDO is the structural analysis for evaluating structural capacity. Structural capacity is related to the maximum values of relative lateral displacement of stories (drift). In this research, static nonlinear pushover analysis with constant displacement coefficient (Council, B.S.S., 2000) is used to measure nonlinear seismic responses of structures. In this method, the structure is loaded with a specific distribution of lateral loads, until the displacement of a specific point of the structure reaches the objective displacement. The objective displacement is obtained from FEMA-350 (Agency, F.E.M., 2013).

$$\delta_t = C_0 C_1 C_2 S_a \frac{T_e^2}{4\pi^2} g \quad (1)$$

where, C_0 relates the spectral displacement of the single degree of freedom (SDOF) system to the roof displacement of the multi-degree of freedom (MDOF) system, C_1 is the correction coefficient of the maximum inelastic displacement of the calculated displacement for linear behavior and C_2 represents the cyclic effect on reducing the members' stiffness and strength. T_e is the effective main period of the structure in the intended direction and S_a is the response spectrum acceleration related to T_e . In this study, static, modal, pushover and time-history analyses are performed using the OpenSees platform (Gu et al., 2010).

According to the code written using MATLAB programming language (MathWorks, 2005), several

limitations have to be taken into consideration during the design process in order to ensure that the obtained designs are applicable and efficient. These limitations can be reviewed in three steps as follows:

First Step: Controlling the Condition of Elements at Connection Areas in Terms of Applicability

- Controlling that the geometric dimensions of each column section are not larger than its lower column:

$$g_{able,2.1.1}(x) = \left(\frac{I_{z,bot}}{I_{z,top}}, \frac{h_{bot}}{h_{top}}, \frac{w_{bot}}{w_{top}}, \frac{t_{w,bot}}{t_{w,top}}, \frac{t_{f,bot}}{t_{f,top}} \right)_i - 1 \leq 0$$

$$i = 1, 2, \dots, n \quad (2)$$

- Controlling that the flange width of each beam is not larger than the flange of the column connected to it:

$$g_{able,2.1.2}(x) = \left(\frac{W_{beam}}{W_{column}} \right)_i - 1 \leq 0$$

$$i = 1, 2, \dots, n \quad (3)$$

- Controlling the criteria of special ductility according to FEMA-350 for sections:

$$g_{able,2.1.3.1}(x) = \left(\frac{b}{t} \right)_i - 1 \leq 0 \quad i = 1, 2, \dots, n$$

$$0.32 \sqrt{\frac{E}{R_y F_y}} \quad (4)$$

$$g_{able,2.1.3.2}(x) = \begin{cases} \left(\frac{b}{t} \right)_i - 1 \leq 0; & \text{Columns} \\ 1.57 \sqrt{\frac{E}{R_y F_y}} & \\ \left(\frac{b}{t} \right)_i - 1 \leq 0; & \text{Beams} \\ 2.57 \sqrt{\frac{E}{R_y F_y}} & \end{cases} \quad i = 1, 2, \dots, n \quad (5)$$

- Controlling structure columns for minimum slenderness:

$$g_{able,2.1.3.1}(x) = \left(\frac{KL}{r} \right)_i - 1 \leq 0 \quad i = 1, 2, \dots, n \quad (6)$$

$$g_{grav,2.2}(x) = \begin{cases} \frac{P_u}{2\phi_c P_n} + \left(\frac{M_{ux}}{\phi_b M_{nx}} + \frac{M_{uy}}{\phi_b M_{ny}} \right) - 1 \leq 0 & \text{for } \frac{P_u}{\phi_c P_n} < 0.2 \\ \frac{P_u}{\phi_c P_n} + \frac{8}{9} \left(\frac{M_{ux}}{\phi_b M_{nx}} + \frac{M_{uy}}{\phi_b M_{ny}} \right) - 1 \leq 0 & \text{for } \frac{P_u}{\phi_c P_n} \geq 0.2 \end{cases} \quad i = 1, 2, \dots, ne \quad (8)$$

where, P_u is the required (tensile or compressive) strength, P_n is the nominal axial resistance (tensile or compressive), 0.9 for tension and 0.85 for compression, ϕ_c is the compression strength coefficient, M_{ux} and M_{uy} are the required bending strengths around x and y axes,

x is the vector of design variable, n is the number of joints having column connection of beam-to-column connection and I_g , h , w , t_w and t_f are: the moment of inertia around bending axis (perpendicular to structure plan), height, flange width, column web and flange thicknesses, respectively. Also, w_{beam} and w_{column} are the flange width of beam and column, respectively. E (=210 GPa) is the Young's modulus, F_y (=235 MPa) is the material yielding stress, K is the effective length coefficient, L is the free length and r is the gyration radius around the bending axis (perpendicular to structure plane). The values in parentheses are the values having been used in the present research.

Step Two: Controlling Serviceability

The structure is reviewed for gravity loads. To perform the control, the following load combinations (Q_G^{SC}) are considered:

$$Q_G^{SC} = \begin{cases} 1.4Q_D \\ 1.2Q_D + 1.6Q_L \end{cases} \quad (7)$$

Q_D (=9.8067kN/m) and Q_L (=24.5166kN/m) are respectively the effective dead and live loads exerted on the structure. This operation is carried out under the control of the LRFD-AISC (Paikowsky, 2002) for non-seismic load combinations in all structural members, as follows:

M_{nx} and M_{ny} are the nominal bending strengths around x and y axes and ϕ_b is the bending strength coefficient.

Step Three: Performance-based Design

The functional concept of PBD is a displacement-based design approach, in which design criteria and the

amount of required capacity are expressed based on the amount of displacement (not the amount of force) (Sullivan, 2003). To achieve performance-based control, the relative displacement of stories should be determined at different performance levels by using pushover analysis. For conducting the above analysis, gravity loads are considered in accordance with (Provisions, 1997) and are as follows:

$$Q_G^{PBD} = 1.1(Q_D + Q_L) \quad (9)$$

S_a at two performance levels of IO and CP is used from the spectrum response of Iranian standard no. 2800 (code of practice for earthquake-resistant design of buildings) (Iranian Standard 2800) at the design earthquake level (LS) and the resulting acceleration has been scaled for the probabilities of 50% and 2% in 50 years, respectively at IO and CP performance levels:

$$S_a^{LS} = ABI \quad (10)$$

$$B = B_1 N \quad (11)$$

$$B_1 = \begin{cases} S_0 (= 1.1) + (S - S_0 + 1) \frac{T}{T_0} = 1.1 + 11T & ; \quad 0 < T < T_0 (= 0.15s) \\ (S + 1) \frac{T_s}{T} = \frac{1.925}{T} & ; \quad T > T_s \\ S (= 1.75) + 1 = 2.75 & ; \quad T_0 < T < T_s (= 0.7s) \end{cases} \quad (12)$$

$$N = \begin{cases} 1 & ; \quad T < T_s \\ \frac{0.7}{4 - T_s} (T - T_s) + 1 & ; \quad T_s \leq T \leq 4s \\ 1.7 & ; \quad T > 4s \end{cases} \quad (13)$$

$$S_a^{IO} = S_a^{LS} \times \left(\frac{75}{475} \right)^{0.44} \approx 0.4439 S_a^{LS} \quad (14)$$

$$S_a^{CP} = S_a^{LS} \times \left(\frac{2475}{475} \right)^{0.29} = 1.61 S_a^{LS} \rightarrow S_a^{CP} = 1.5 S_a^{LS} \quad (15)$$

$A(=0.35)$ is the structure acceleration to gravity acceleration ratio, B is the structure response coefficient, B_1 is the base response coefficient, N is the distance to fault coefficient, $I(=1.2)$ is the importance coefficient and S_a^{IO} , S_a^{LS} and S_a^{CP} are the spectral accelerations corresponding to IO, LS and CP performance levels, respectively.

After calculating the objective displacement, performing pushover analysis and finding story drifts at the performance levels of IO (D_{IO}) and CP (D_{CP}), it is necessary to calculate the structural confidence levels at the IO and CP performance levels according to FEMA-350 as follows. Based on this guideline, they should not be less than 50% and 90%, respectively:

$$(confidence_level)_{IO} = CDF\left('Normal', \frac{k\beta_{UT}}{2} - \frac{Ln(\lambda_{IO})}{\beta_{UT}}\right) \geq 50\% \quad (16)$$

$$(confidence_level)_{CP} = CDF\left('Normal', \frac{k\beta_{UT}}{2} - \frac{Ln(\lambda_{CP})}{\beta_{UT}}\right) \geq 90\% \quad (17)$$

where, β_{UT} is the uncertainty parameter, k (=4) is the region risk curve slope and λ is the certainty subscript that is calculated from the following equation:

$$\lambda_i = \left(\frac{\gamma \times \gamma_a \times D}{\phi \times C}\right)_i ; \quad i = IO, CP \quad (18)$$

γ is the model precision coefficient, γ_a is the analysis uncertainty coefficient, ϕ is the strength uncertainty coefficient and C is the structure general drift capacity.

It should be noted that the FEMA-350 has presented four criteria of total drift, local drift, tensile control at the place of column patches and compression control of columns to accept steel moment-resisting frames. These criteria have been reviewed in previous studies (Fragiadakis et al., 2006; Gholizadeh et al., 2013; Gholizadeh, 2015) and in the present study, indicating the absolute rule of thumb of the general drift criterion over the three other criteria, so that if the general drift is satisfied, the values of the other criteria have a clear distance from the certainty level introduced in this code.

- Controlling structure certainty level at the IO and CP performance levels:

$$g_{PBD,2.3.1.1}(x) = \frac{50\%}{(confidence_level)_{IO}} - 1 \leq 0 \quad (19)$$

$$g_{PBD,2.3.1.2}(x) = \frac{90\%}{(confidence_level)_{CP}} - 1 \leq 0 \quad (20)$$

- Controlling the seismic rule of strong column-weak beam (SCWB):

$$g_{SCWB}(x) = \frac{\sum_{i=1}^n M_C^{Beams}}{\sum_{i=1}^m M_C^{Columns}} - 1 \leq 0 \quad (21)$$

n and m are the number of beams and columns connected to each node of the structure, respectively and M_C^{Beams} and $M_C^{Columns}$ are respectively the beam and column plastic moments that are derived from the following relations:

$$M_C^{Beams} = C_{pr} R_y Z_b F_y + \left(\frac{2Z_b}{L'} + \frac{\omega L'}{2F_y}\right) \times \frac{d_c + d_b}{2} F_y \quad (22)$$

$$M_C^{Columns} = Z_c F_y \left(1 - \frac{P_u}{A_g F_y}\right) \quad (23)$$

Z_b and Z_c are the beam and column plastic modulus and d_b and d_c are the beam and column sections' depth, respectively. ω is the distributed load exerted on the beam according to pushover load combination, L' is the beam net (free) span, A_g is the total section area of column, P_u is the seismic analysis axial force at CP performance level, R_y (=1.1) is the beam material coefficient and C_{pr} is the connection power ratio that is obtained from the following relation:

$$C_{pr} = \frac{F_y + F_u}{2F_y} \quad (24)$$

F_u (=305.5MPa) is the steel ultimate stress.

QUASI-OBJECTIVE FUNCTION

The initial cost of a structure for moment-resisting steel frames is completely a function of the structure weight; thus, the quasi-objective function is defined as follows:

$$\Phi(x, r_p) = \sum_{i=1}^{ng} \rho_i A_i \sum_{j=1}^{nm} L_j \left(1 + r_p \sum_{k=1}^{nc} (\max(0, g_k(x)))^2\right) \quad (25)$$

ρ_i and A_i are weight per unit volume and section area of the i^{th} population, respectively, nm is the number of members of the i^{th} population, L_j is the length of element j in the i^{th} population, $g_k(x)$ is the k^{th} behavioral

constraint, n_c is the number of constraints and r_p is the increasing penalty parameter. In this paper, the member sections are selected using optimization algorithm and are shown in Table 1.

Table 1. Available W-sections

Columns				Beams			
No.	Profile	No.	Profile	No.	Profile	No.	Profile
1	W14×48	13	W14×257	1	W12×19	13	W21×50
2	W14×53	14	W14×283	2	W12×22	14	W21×57
3	W14×68	15	W14×311	3	W12×35	15	W24×55
4	W14×74	16	W14×342	4	W12×50	16	W21×68
5	W14×82	17	W14×370	5	W18×35	17	W24×62
6	W14×132	18	W14×398	6	W16×45	18	W24×76
7	W14×145	19	W14×426	7	W18×40	19	W24×84
8	W14×159	20	W14×455	8	W16×50	20	W27×94
9	W14×176	21	W14×500	9	W18×46	21	W27×102
10	W14×193	22	W14×550	10	W16×57	22	W27×114
11	W14×211	23	W14×605	11	W18×50	23	W30×108
12	W14×233	24	W14×665	12	W21×44	24	W30×116

Neural Network (NN)

According to the high number of pushover computing loads in the present study, in order to adjust the run time, it is used from the neural networks BP (Wang et al., 2018) and RBF (Basu et al., 2018) for estimating D_{IO} and D_{CP} without performing pushover analysis.

The input variables of the neural networks include the number of members' sections and the 3, 6 or 12 first periods of respectively the 3, 6 and 12-story frames and their output is D_{IO} and D_{CP} , respectively. In order to train the BP neural network for 3, 6 and 12-story frames, a number of 240, 320 and 400 training pairs were used and

a number of 60, 80 and 100 testing pairs were also used for testing, respectively and the most appropriate number of neurons for its only intermediate layer was obtained as equal to 9, 13 and 9 neurons, respectively. A number of 300, 400 and 500 training pairs were also used for training RBF network in 3, 6 and 12-story frames, respectively. The results from calculating the Absolute Percentage Error (APE) and the Mean Absolute Percentage Error (MAPE) represent the absolute superiority of BP to RBF; hence, it is used from BP network in the above research. MAPE for BP network is shown in Figure 1. The statistical parameters of the RBF network's absolute errors are given in Table 2.

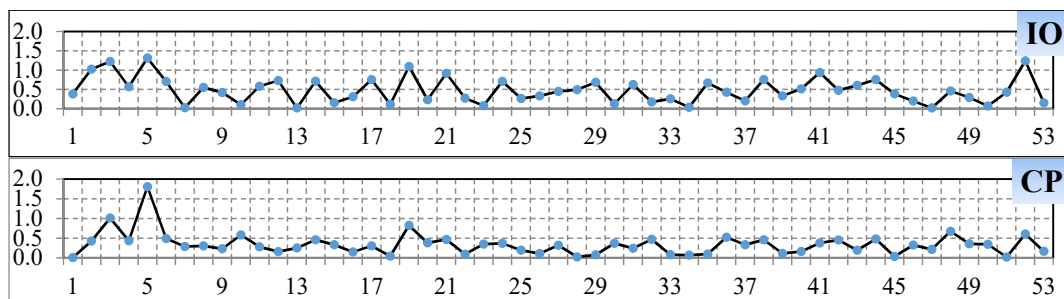


Figure (1): BP network's MAPE

Table 2. Statistical parameters of the RBF network's absolute errors

Story Num.	Performance Level	Mean ABS err.	Max. ABS err.	Std. ABS err.
3	IO	0.5%	20.4%	2.4%
	CP	3.6%	13.6%	2.3%
6	IO	2.2%	13.0%	1.8%
	CP	4.5%	22.5%	3.3%
12	IO	2.5%	11.3%	1.6%
	CP	5.3%	17.4%	4.1%

CALCULATING COLLAPSE MARGIN RATIO

Considering the new attitude to the analysis process and designing of high-rise buildings, it is raised from the related regulations that a performance-based seismic design in such structures requires that the provision of performance objectives during a rare or sequential seismic event is particularly evaluated. One of the important challenges in this method is the choice of an effective analysis approach that is applied to analyze the structural model, based on which the distribution of seismic requirements is obtained, which by a precise and complete evaluation of the subject, requires an Incremental Dynamic Analysis (IDA) at different levels of fragmentation. This method utilizes the fundamental concept of "acceleration record" and within its definition, the structure behavior can be evaluated from the elastic region to the threshold of collapse.

In summary, in the IDA analysis, the structural model is subjected to a set of earth acceleration records that are scaled at multiple levels. The result of IDA analysis at these levels is plotted as the variations in seismic requirements in terms of the characteristic stimulation parameter, where the above process is called fragility analysis and the resulting diagrams are called fragility curves. One of the important purposes and applications of fragility analysis and its curve development is the safety assessment of a structure that is defined in the form of a collapse margin ratio (CMR). Figure 2 schematically illustrates the curve of structure capacity, in which the pseudo-acceleration spectrum (S) and total structural displacement index (SD) are used instead of base shear force and displacement in the roof level (Council, A.T., 2009).

The above equivalence is performed based on the assumption that 100% of the effective mass of the structure contributes in the structure main mode with the main period T. Also, S_{MT} is the symbol of quasi-acceleration of the MCE earthquake spectrum and \hat{S}_{CT} is the pseudo-acceleration of the earthquake spectrum that causes the structure to collapse in 50% of cases and, in other words, represents the mean value of the pseudo-acceleration of the earth motion at the collapse level. As can be seen, this motion is at a higher level than the MCE earthquake level and for this reason, an earthquake at the MCE level will lead to structure collapse with less chance. Therefore, the safety margin of a structure against collapsing is defined as follows:

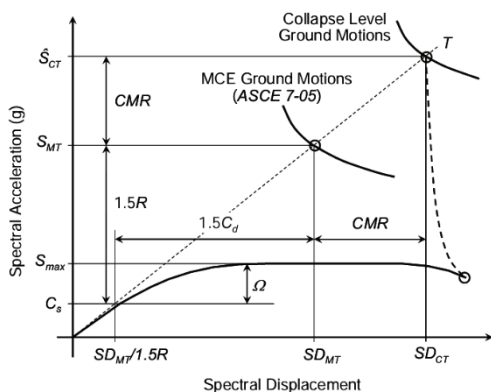


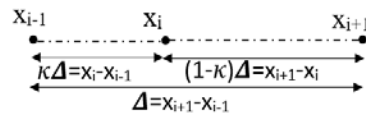
Figure (2): Displaying the margin of safety of a structure based on the normalized capacity curve

$$CMR = \frac{\hat{S}_{CT}}{\hat{S}_{MT}} = \frac{\hat{S}D_{CT}}{\hat{S}D_{MT}} \quad (26)$$

In other words, the safety margin indicates that \hat{S}_{MT} should be multiplied by several times, so that 50% of the ground motions cause the structure to collapse. Obviously, the CMR value for a structural system is dependent on the uncertainties arising from the stimulation nature and the modeling approach (Council, A.T., 2009).

(FDA) METAHEURISTIC OPTIMIZATION ALGORITHM

Certainly, for a one-dimensional function $y = f(X)$, the value of X^* is a minimum for the function when: $f'(X^*) = 0$ and $f''(X^*) > 0$. Thus, the root of equation $f'(X) = 0$ is an overall optimum for function $y = f(X)$.



One of the best iteration ways to find the root of equations such as $f'(X) = 0$, is the Newton-Raphson method:

$$X_i^{t+1} = X_i^t - \frac{f'(X_i^t)}{f''(X_i^t)} \quad (27)$$

Accordingly, calculating the form of the quasi-objective m-dimensional function and the values of its first and second derivatives, even by having its explicit form, is a difficult and nearly impossible task; however, instead of calculating the explicit values of its derivations, it can be used from finite differences for calculating the approximate numerical value of its derivations in different conditions of X .

If X_{i-1} , X_i and X_{i+1} are three sequential members of the population, assuming that $f(X_{i+1}) > f(X_i) > f(X_{i-1})$:

$$\Rightarrow \begin{cases} X_i - X_{i-1} = \kappa(X_{i+1} - X_{i-1}) \\ X_{i+1} - X_i = (1 - \kappa)(X_{i+1} - X_{i-1}) \end{cases} \quad \kappa < 1 \quad (28)$$

By inserting $f(x_{i-1}) = f_{i-1}$, $f(x_i) = f_i$ and $f(x_{i+1}) = f_{i+1}$, if α is the slope of the connector line between two points and β is the slope of the tangent to the curve, as shown in Figure 3,

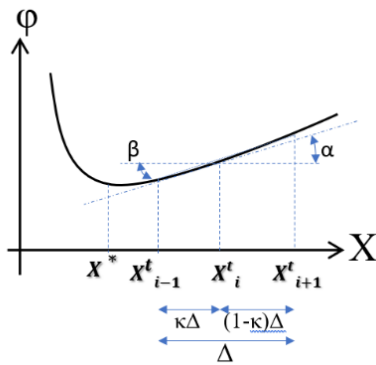


Figure (3): Finite difference algorithm

$$\alpha \approx \beta \rightarrow f'(X_i) \approx \frac{f_{i+1} - f_{i-1}}{X_{i+1} - X_{i-1}} \quad (29)$$

$$f''(X_i) \approx \frac{f'_i - f'_{i-1}}{X_{i+1} - X_{i-1}} \quad (30)$$

$$f''(X_i) \approx \frac{\frac{f_{i+1} - f_i}{(1 - \kappa)(X_{i+1} - X_{i-1})} - \frac{f_i - f_{i-1}}{\kappa(X_{i+1} - X_{i-1})}}{X_{i+1} - X_{i-1}} \quad (31)$$

$$f''(X_i) \approx \frac{1}{\kappa(1 - \kappa)} \frac{\kappa f'_{i+1} - f'_i + (1 - \kappa)f'_{i-1}}{(X_{i+1} - X_{i-1})^2} \quad (32)$$

Using the Newton-Raphson method (27) for optimizing a function such as $f(x)$ and starting an

iteration method by substituting (29) and (32) in it and given that:

$$\text{Subs. (29)\&(32)to(27): } X_i^{t+1} = X_i^t - \frac{\frac{f_{i+1}^t - f_{i-1}^t}{X_{i+1}^t - X_{i-1}^t}}{\frac{1}{\kappa(1-\kappa)} \frac{\kappa f_{i+1}^t - f_i^t + (1-\kappa)f_{i-1}^t}{(X_{i+1}^t - X_{i-1}^t)^2}} \quad (33)$$

$$\Rightarrow X_i^{t+1} = X_i^t - \kappa(1-\kappa) \frac{f_{i+1}^t - f_{i-1}^t}{\kappa f_{i+1}^t - f_i^t + (1-\kappa)f_{i-1}^t} (X_{i+1}^t - X_{i-1}^t)$$

$$\text{grad}_i^{t+1} = -\kappa(1-\kappa) \frac{f_{i+1}^t - f_{i-1}^t}{\kappa f_{i+1}^t - f_i^t + (1-\kappa)f_{i-1}^t} \quad (34)$$

Equation (33), with the weight ratio of the current iteration number (*CurrIter*) to the total iteration (*TotIter*), includes exploitation in finding the optimal point of the function to avoid local optimization and to make exploration:

$$SX_i^{t+1} = X_i^t - r \otimes \text{grad}_i^{t+1} \left(1 - \frac{\text{CurrIter}}{\text{TotIter}}\right) (X_{i+1}^t - X_{i-1}^t) - \frac{\text{CurrIter}}{\text{TotIter}} (X_i^t - X_{i-1}^t) \quad (35)$$

where, *r* is a random vector whose arrays equal the number of the variables of *f* and \otimes is an array-to-array multiplication. In order to prevent the prolongation of the paper, description of the well-known algorithms of PSO, ECBO and FA is not included. The pseudo-code of the algorithm is shown in Figure 4. The flowchart for implementing this algorithm is depicted in Figure 5.

Finite Difference Algorithm

```

Pseudo objective function  $\Phi(X, rp)$ 
Initialize the FiniteDifferences (FD) population  $X_i$  ( $i=1, \dots, np$ ) on a random basis
Initialize  $rp$  by a constant value
Define the grad sensitive coefficient
while ( $k < \text{maximum number of generations for outer loop (Iter)}$ )
  while ( $n < \text{maximum number of generations for inner loop (np)}$ )
    Determine the best FD
    if  $\Phi(FDi) > \Phi(FDj)$ 
      Compute grad between  $FDi$ ,  $F Dj$  and the best  $FD(\text{gradi})$ 
      Generate a new population by updating positions of the previous population
      Update the attractiveness of each  $F Ds$ 
      Rank the  $F Ds$  and find the best solution  $X^*$ 
    end while
  Initialize a new population by selecting  $F Ds$  from the vicinity of  $X^*$ 
  Repeat the inner loop
  Update the best solution  $X^*$ 
end while
Present the final solution
    
```

Figure (4): Pseudo-code for FDA

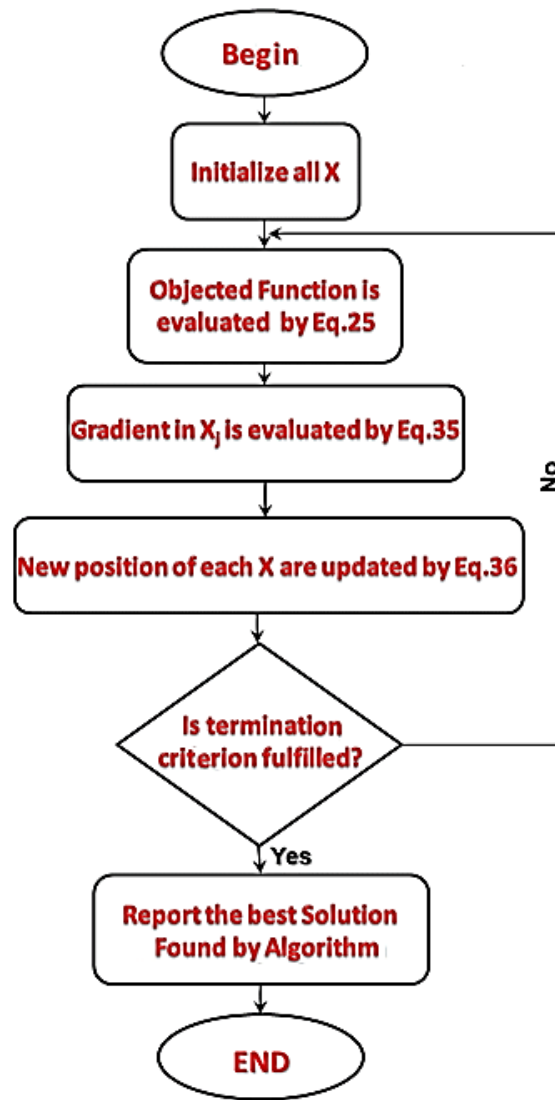


Figure (5): Flowchart of FDA

RELIABILITY OF THE OPTIMIZED FRAMES

To calculate the reliability of the optimized frames, the LatinHyperCube sampling method was used with 10^6 samples for each frame. The probabilistic variables F_y and E , the strain hardening H and s_a^{IO} and s_a^{CP} are considered in accordance with the specifications given in Table 3. Inter-story drift of each frame is determined

with 10^6 samples of probabilistic variables and evaluated by the BP neural network; each sample is known to be an acceptable sample within the FEMA-350 range. If N_s is the number of acceptable samples and $N(= 10^6)$ is the total number of samples, the reliability is obtained by using the following equation:

$$reliability = \frac{N_s}{N} \times 100\% \tag{36}$$

Table 3. Statistical data of probabilistic variables

Variable	Mean	Coefficient of variation	Distribution function
Fy	235MPa	5%	Normal
E	210Gpa	5%	Normal
H	0.03	5%	Log-Normal
S_a^{10}	$0.4439S_a^{LS}$	10%	Gumbel
S_a^{CP}	$1.5S_a^{LS}$	10%	Gumbel

NUMERICAL EXAMPLES

In this section, 3 ,6 and 12-story moment-resisting steel frames with special ductility, as shown in Figure 6, are optimized by PBDO approach and using four algorithms based on initial cost objective function and by the help of BP neural network. Thereafter, the reliability and CMR values are calculated for each

optimized frame according to FEMA-P695 and by IDA analysis and fill&hunt pattern to find collapsing. The obtained results for 3 ,6 and 12-story frames are presented in Tables 4, 5 and 6, respectively. In addition, IDA curves for the 3 ,6 and 12-story frames are respectively shown in Figures 7-9. Fragility curves for the 3 ,6 and 12-story frames are respectively shown in Figures 10-11.

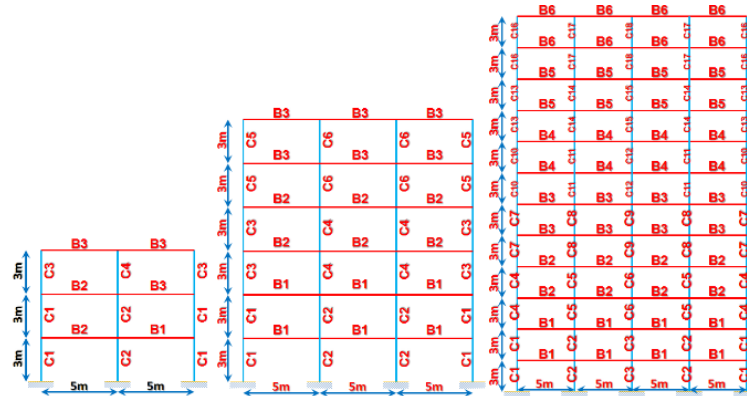


Figure (6): Numerical examples

Table 4. PBD optimization, reliability and CMR results for 3-story SMF

Design variables	Algorithm			
	PSO	ECBO	FA	FDA
C ₁	W14×53	W14×48	W14×48	W14×53
C ₂	W14×68	W14×74	W14×74	W14×68
C ₃	W14×48	W14×48	W14×48	W14×48
C ₄	W14×53	W14×48	W14×48	W14×48
B ₁	W12×22	W12×22	W12×22	W12×22
B ₂	W12×22	W12×22	W12×22	W12×22
B ₃	W12×19	W12×22	W12×22	W12×19
θ_{10}^{max}	0.012561	0.012701	0.012701	0.012569
θ_{CP}^{max}	0.04011	0.040155	0.040155	0.040177
Weight(kg)	3152.9026	3139.7633	3139.7633	3130.1616
Reliability	50.02%	49.49%	49.49%	51.37%
CMR	3.3917	3.2612	3.2612	3.2799

Table 5. PBD optimization, reliability and CMR results for 6-story SMF

Design variables	Algorithm			
	PSO	ECBO	FA	FDA
C ₁	W14×68	W14×68	W14×68	W14×68
C ₂	W14×82	W14×82	W14×82	W14×82
C ₃	W14×68	W14×68	W14×68	W14×68
C ₄	W14×74	W14×74	W14×82	W14×82
C ₅	W14×68	W14×68	W14×68	W14×53
C ₆	W14×68	W14×68	W14×68	W14×68
B ₁	W18×35	W18×35	W18×35	W18×35
B ₂	W18×35	W18×35	W18×35	W18×35
B ₃	W12×22	W12×22	W12×22	W12×22
θ_{IO}^{max}	0.0095072	0.0095072	0.0094626	0.0093342
θ_{CP}^{max}	0.032682	0.032682	0.032725	0.032333
Weight(kg)	11734.3158	11734.3158	11867.7293	11600.9025
Reliability	31.22%	31.22%	28.67%	34.56%
CMR	2.5030	2.5030	2.2003	2.5857

Table 6. PBD optimization, reliability and CMR results for 12-story SMF

Design variables	Algorithm			
	PSO	ECBO	FA	FDA
C ₁	W14×132	W14×82	W14×132	W14×132
C ₂	W14×145	W14×145	W14×145	W14×145
C ₃	W14×159	W14×159	W14×159	W14×159
C ₄	W14×82	W14×82	W14×82	W14×82
C ₅	W14×132	W14×132	W14×132	W14×132
C ₆	W14×145	W14×145	W14×145	W14×145
C ₇	W14×68	W14×68	W14×74	W14×68
C ₈	W14×132	W14×132	W14×132	W14×132
C ₉	W14×132	W14×132	W14×132	W14×132
C ₁₀	W14×68	W14×68	W14×68	W14×68
C ₁₁	W14×82	W14×82	W14×82	W14×82
C ₁₂	W14×82	W14×82	W14×82	W14×82
C ₁₃	W14×53	W14×53	W14×53	W14×53
C ₁₄	W14×68	W14×68	W14×68	W14×68
C ₁₅	W14×68	W14×68	W14×68	W14×68
C ₁₆	W14×48	W14×48	W14×48	W14×48
C ₁₇	W14×48	W14×48	W14×48	W14×48
C ₁₈	W14×68	W14×68	W14×68	W14×53
B ₁	W16×45	W18×40	W16×45	W16×45
B ₂	W16×50	W16×50	W16×50	W16×50
B ₃	W16×45	W16×45	W16×45	W16×45
B ₄	W18×35	W18×35	W18×35	W18×35
B ₅	W12×35	W12×35	W12×35	W12×35
B ₆	W12×19	W12×19	W12×19	W12×19
θ_{IO}^{max}	0.010404	0.010281	0.010404	0.010389
θ_{CP}^{max}	0.038824	0.038197	0.038824	0.038828
Weight (kg)	38319.9702	37119.2495	38319.9702	38186.5567
Reliability	47.74%	43.28%	47.74%	48.70%
CMR	2.3590	2.3226	2.3590	2.3597

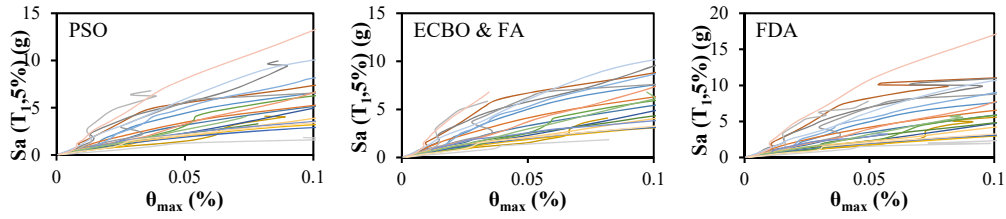


Figure (7): 3-story IDA curves

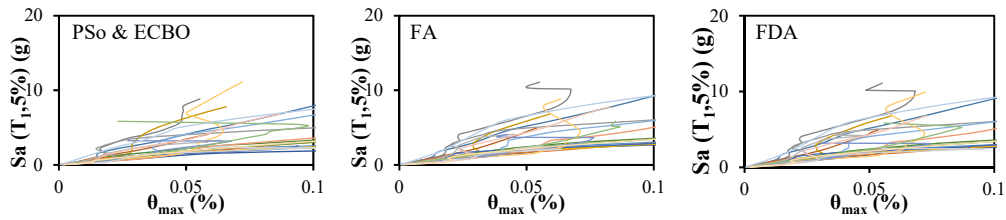


Figure (8): 6-story IDA curves

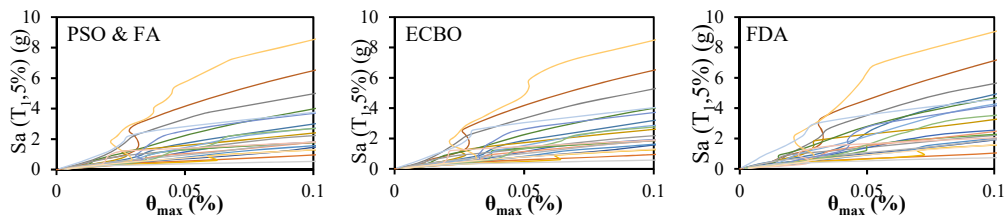


Figure (9): 12-story IDA curves

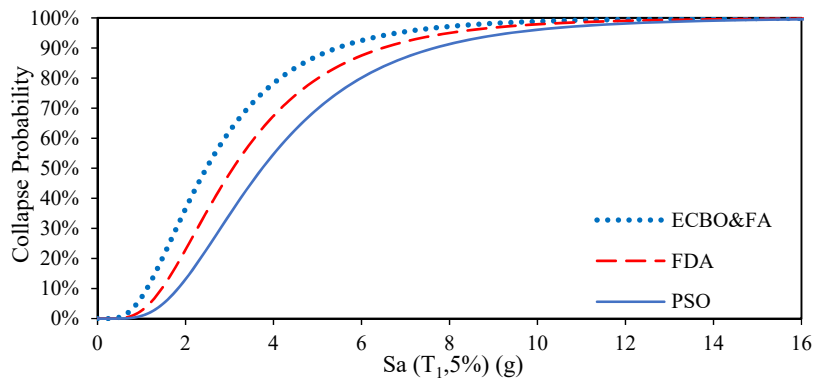


Figure (10): 3-story fragility curves

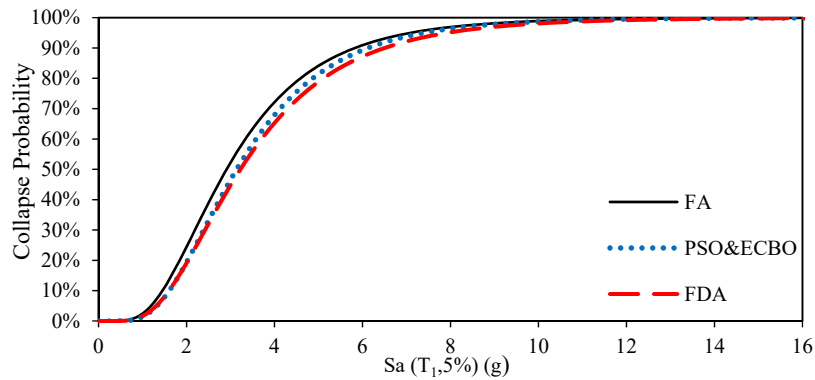


Figure (11): 6-story fragility curves

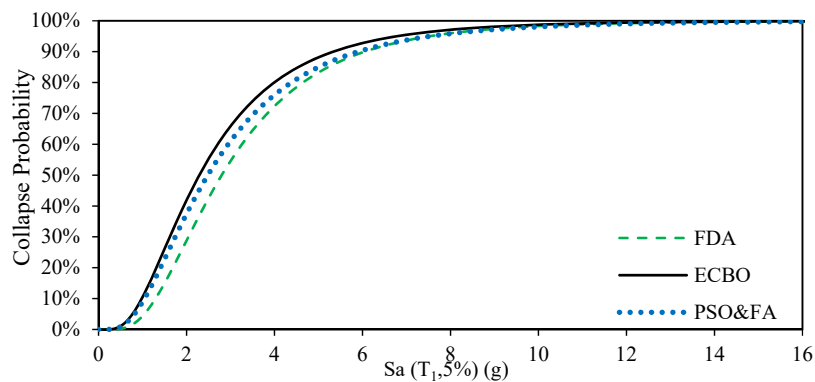


Figure (12): 12-story fragility curves

SUMMARY AND CONCLUSIONS

By evaluating the reliability and CMR results for the performance-based optimized frames and with the initial cost objective function, it is clear that they are of higher CMR than the FEMA-P695 allowed limit; however, according to the ductility and importance considered for them, not much certainty in future strong earthquakes is provided. Thus, the probability of serious damages to the frames during severe earthquakes and a significant increase in the lifecycle cost of the structure is very high.

In order to reduce the cost of the lifecycle for short, medium and tall moment-resisting steel frames with special ductility and high relative importance, the following two solutions are suggested:

- If performance-based optimization is performed, the objective function is necessarily the lifecycle cost.

Although this is more likely to increase the initial cost, it will raise CMR, trusting the structure in future possible severe earthquakes.

- If the optimization objective function is the initial cost or the need for CMR is high due to high relative importance, the optimization is better to be performed based on reliability and RBDO approach. It is clear that frames designed by this method will be of a higher reliability than frames designed by the previous method. Definitely, RBDO optimization is very time-consuming with heavy computational load, even when using soft computing techniques such as neural networks. In order to avoid this heavy computational load, optimization can be carried out by initial cost objective function using PBDO; however, a more acceptable level of CMR is required to be added as a new constraint to other constraints.

With regards to the last suggestion, two major points must be specified:

The first point is the acceptable level of CMR for the structure. The basic solution could be calculating the CMR of optimized frames based on reliability (RBDO) and with the structure lifecycle cost objective function and selecting a general criterion from finite examples (given the heavy volume of calculations) for the entire system of moment-resisting steel frames. The second

point is to calculate CMR for each member of the optimization population in each iteration, which is very time-consuming due to the high number of iterations of various optimization algorithms and the large volume of CMR computations, which imposes a high computational load on the algorithm. The neural network can also be used to calculate the CMR of the population members, in order to overcome this problem.

REFERENCES

- Agency, F.E.M. (2013). "Recommended seismic design criteria for new steel moment-frame buildings". FEMA 350.
- Basu, S. et al. (2018). "Deep neural networks for texture classification—a theoretical analysis". *Neural Networks*, 97, 173-182.
- Council, A.T. (1996). "Seismic evaluation and retrofit of concrete buildings". 2. Appendices, ATC.
- Council, A.T. (2009). "Quantification of building seismic performance factors". US Department of Homeland Security, FEMA.
- Council, B.S.S. (2000). "Prestandard and commentary for the seismic rehabilitation of buildings". Report FEMA-356, Washington, DC.
- FEMA, A. (2005). "440, improvement of nonlinear static seismic analysis procedures". FEMA-440, Redwood City.
- Fragiadakis, M., and Lagaros, N.D. (2011). "An overview to structural seismic design optimisation frameworks". *Computers and Structures*, 89 (11-12), 1155-1165.
- Fragiadakis, M., Lagaros, N.D., and Papadrakakis, M. (2006). "Performance-based multiobjective optimum design of steel structures considering life-cycle cost". *Structural and Multidisciplinary Optimization*, 32 (1), 1.
- Gholizadeh, S. (2015). "Performance-based optimum seismic design of steel structures by a modified firefly algorithm and a new neural network". *Advances in Engineering Software*, 81, 50-65.
- Gholizadeh, S., and Milany, A. (2018). "An improved fireworks algorithm for discrete sizing optimization of steel skeletal structures". *Engineering Optimization*, 1-21.
- Gholizadeh, S., Kamyab, R., and Dadashi, H. (2013). "Performance-based design optimization of steel moment frames". *Int. J. Optim. Civil Eng.*, 3, 327-343.
- Gu, Q., Conte, J., and Barbato, M. (2010). "OpenSees command language manual response sensitivity analysis based on the direct differentiation method (DDM)". Berkeley, CA: Pacific Earthquake Engineering Center, University of California.
- Kaveh, A. et al. (2010). "Performance-based seismic design of steel frames using ant colony optimization". *Journal of Constructional Steel Research*, 66 (4), 566-574.
- Kaveh, A., and Ghazaan, M.I. (2014). "Enhanced colliding bodies optimization for design problems with continuous and discrete variables". *Advances in Engineering Software*, 77, 66-75.
- Kaveh, A., and Ghazaan, M.I. (2017). "Enhanced whale optimization algorithm for sizing optimization of skeletal structures". *Mechanics-based Design of Structures and Machines*, 45 (3), 345-362.
- Kaveh, A., and Mahdavi, V. (2014). "Colliding bodies optimization: a novel meta-heuristic method". *Computers and Structures*, 139, 18-27.
- Kaveh, A., and Mahdavi, V. (2014). "Colliding bodies optimization method for optimum discrete design of truss structures". *Computers and Structures*, 139, 43-53.

- Kaveh, A., and Nasrollahi, A. (2014). "Performance-based seismic design of steel frames utilizing charged system search optimization". *Applied Soft Computing*, 22, 213-221.
- Kaveh, A., Fahimi-Farzam, M., and Kalateh-Ahani, M. (2015). "Performance-based multi-objective optimal design of steel frame structures: nonlinear dynamic procedure". *Scientia Iranica*, 22 (2), 373-387.
- Kaveh, A., Laknejadi, K., and Alinejad, B. (2012). "Performance-based multi-objective optimization of large steel structures". *Acta Mechanica*, 223 (2), 355-369.
- Liu, Z., Atamturktur, S., and Juang, C.H. (2013). "Performance-based robust design optimization of steel moment-resisting frames". *Journal of Constructional Steel Research*, 89, 165-174.
- MathWorks, I. (2005). "MATLAB: the language of technical computing". *Desktop Tools and Development Environment, Version 7. Vol. 9. MathWorks.*
- Neighbors, C. et al. (2012). "Sensitivity analysis of FEMA HAZUS earthquake model: case study from King County, Washington". *Natural Hazards Review*, 14 (2), 134-146.
- Paikowsky, S.G. (2002). "Load and resistance factor design (LRFD) for deep foundations". *Foundation Design Codes—Proceedings of IWS Kamakura*, 59-94.
- Provisions, B.P.o.I.S.S. (1997). "NEHRP recommended provisions for seismic regulations for new buildings and other structures: provisions". 302, FEMA.
- Safety, I.S. "NEHRP recommended provisions for seismic regulations for new buildings and other structures". FEMA 450.
- Standard, I., 2800. "Seismic-resistant design of buildings code of practice".
- Sullivan, T. et al. (2003). "The limitations and performances of different displacement based design methods". *Journal of Earthquake Engineering*, 7 (spec01), 201-241.
- Wang, F., Liu, H., and Cheng, J. (2018). "Visualizing deep neural network by alternately image blurring and deblurring". *Neural Networks*, 97, 162-172.